ChemComm

Accepted Manuscript

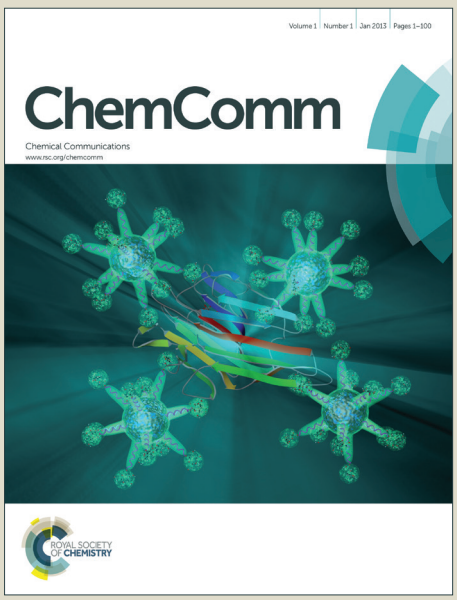

ROYAL SOCIETY OF CHEMISTRY

www.rsc.org/chemcomm

ChemComm

COMMUNICATION

Tuning the Ising-type anisotropy in trigonal bipyramidal Co(II) complexes

Received 00th January 20xx,
Accepted 00th January 20xx

DOI: 10.1039/x0xx00000x

www.rsc.org/

Feng Shao,[a] Benjamin Cahier,[a] Nathalie Guihéry,[b] Eric Rivière,[a] Régis Guillot,[a] Anne-Laure Barra,[c] Yanhua Lan,[d] Wolfgang Wernsdorfer,[d] Victoria E. Campbell,*[a] and Talal Mallah*[a]

This paper demonstrates the engineering and tuning of Ising-type magnetic anisotropy in trigonal bipyramidal Co(II) complexes. Here, we predict that employing a ligand that forces a trigonal bipyramidal arrangement and has weak equatorial σ-donating atoms, increases (in absolute value) the negative zero field splitting parameter *D*. With these considerations in mind, we used a sulfur containing ligand (NS_3^{iPr}), which imposes a trigonal bipyramidal geometry to the central Co(II) ion with long equatorial Co-S bonds. The resulting complex exhibits a larger anisotropy barrier and a longer relaxation time in comparison to the complex prepared with a nitrogen containing ligand (Me_6tren).

Single molecule magnets (SMMs) have been extensively studied in the past 20 years.[1, 2] The interest for these molecules lies in their magnetic bistability, which could have potential applications in quantum information.[3, 4]
The first SMMs were polynuclear transition metal clusters with large zero field splitting (*D*) and large spin ground states (*S*).[1, 5] More recently, research efforts have focused on building mononuclear SMMs with the intent to better control and tune the anisotropy of these systems. There are many examples in the literature of mononuclear lanthanide ion SMMs.[6-8] These complexes benefit from the large spin-orbit coupling of the *f*-block elements inherent to the single ion. These orbitals, however, are deeply buried beneath the valence shell, and the control of the symmetry of the molecules by the ligands is difficult in most cases. While it is not difficult to control the symmetry in transition metal ion complexes. There are few examples of mononuclear complexes that contain a single transition metal ion and display slow relaxation of the magnetization. The most notable examples are a linear Fe(I) complex, a tetrahedral Co(II) complex, and a trigonal bipyramidal Co(II) complex.[9-13]
Mononuclear complexes present clear advantages over polynuclear clusters, as they can be easily manipulated in solution and on surfaces, which is a requirement if we want to employ them as single quantum bits in quantum information applications. The interest in mononuclear transition metal SMMs stems from the possibility to more easily control their coordination geometry and in turn tune and shape their magnetic anisotropy.
Our group has previously shown that imposing a trigonal bipyramidal symmetry around Co(II) and Ni(II) cations leads to large Ising-type magnetic anisotropy (negative *D* value).[10] The anisotropy arises from the axial symmetry imposed by the organic ligand Me_6tren. The [Ni(Me_6tren)Cl](ClO_4) complex has a *D* value close to -200 cm^{-1}, due to the quasi first-order spin-orbit coupling.[10] Blocking of the magnetization was not observed because quantum tunneling is large in *S* = 1 systems and because of the presence of a tiny transverse anisotropy due to a dynamic Jahn-Teller effect, which leads to fast relaxation of the magnetization. Slow relaxation of the magnetization and an opening of the hysteresis loop (both parameters are indicative of SMM behavior) were observed in the Co(II) analog ([Co(Me_6tren)Cl](ClO_4), *S* = 3/2), which has a strict C_{3v} symmetry, even though its anisotropy is much weaker than the isostructural Ni(II) analog. This complex exhibits an Ising-type anisotropy.[9] It was found that the zero field splitting parameter *D* changes when the Cl^- is replaced by Br^- (from -8.1 to -4.6 cm^{-1}, respectively). The difference in magnitude was rationalized in terms of the σ/π donating effects of the ligands. Building upon these results we designed the study reported herein.
This paper describes the rationalization behind engineering and tuning of Ising-type magnetic anisotropy in trigonal bipyramidal Co(II) complexes. We predicted that employing

[a] Institut de Chimie Moléculaire et des Matériaux d'Orsay, CNRS, Université Paris Sud, Université Paris Saclay, 91405 Orsay Cedex, France. E-mail: victoria.campbell@u-psud.fr; talal.mallah@u-psud.fr
[b] Laboratoire de Chimie et Physique Quantiques, Université de Toulouse III, 118 route de Narbonne, 31062 Toulouse, France.
[c] Laboratoire National des Champs Magnétiques Intenses, UPR CNRS 3228, Université J. Fourier, 25, avenue des Martyrs, B.P. 166, 38042 Grenoble, France.
[d] Insitut Néel, CNRS, Université Grenoble Alpes, 25 rue des Martyrs, 38042 Grenoble, France.

† Supporting Information. Detail experimental procedures, spectroscopic data, single crystal X-ray data and computational details. CCDC 1061993 contains the supplementary crystallographic data for this paper. These data can be obtained free of charge from the Cambridge Crystallographic Data Centre via http://www.ccdc.cam.ac.uk/Community/Requestastructure. See DOI: 10.1039/x0xx00000x

ligand, which imposes a trigonal bipyramidal arrangement and has weak equatorial σ-donating atoms, increases the negative zero field splitting parameter *D*.

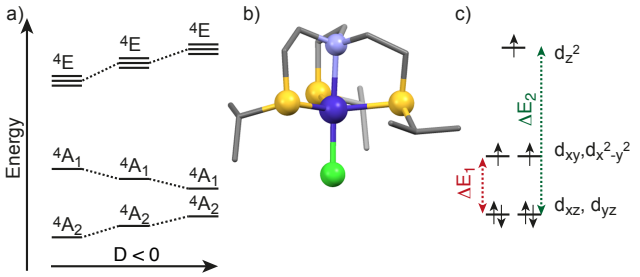

Figure 1. a) Schematic energy diagram of the lowest quadruplets for a trigonal bipyramidal Co(II) complex; b) X-ray crystal structure of [Co(*NS*$_3^{iPr}$)Cl](BPh$_4$): Co = purple; C = grey; N = lilac; S = yellow; Cl = green; H atoms and counter ions were removed for clarity; c) orbital energy diagram for a trigonal bipyramidal Co(II) complex.

We synthesized and magnetically characterized a trigonal bipyramidal Co(II) complex, which was constructed from tris(2-(isopropylthio)ethyl)amine (*NS*$_3^{iPr}$). We show that we can tune the magnitude of *D* by using our design principles and that we can considerably increase *D* (= -23 cm^{-1} for [Co(*NS*$_3^{iPr}$)Cl](BPh$_4$) by lengthening the bonds in the equatorial plane. The magnitude of the anisotropy parameters was experimentally determined and calculated using a correlated *ab initio* method (see SI for details).

From perturbative arguments it can be shown that $|D|$ is inversely proportional to the energy difference between the ground and the excited states.[14, 15] As the symmetry point group of the molecule is close to C$_{3v}$, the rationalization of the magnitude and nature of the Zero-Field Splitting will be performed assuming that the geometry adopts this symmetry (Fig. 1). Two quadruplet excited states, ^{4}A$_1$, and ^{4}E primarily influence the main contributions to the anisotropy parameters. The first excited state ^{4}A$_1$ is responsible for the negative value of *D* while ^{4}E brings a positive but smaller contribution.[9, 13] There is another excited quadruplet state (^{4}A$_2$) just above the ground ^{4}A$_2$ state but it does not contribute to *D* (it does not appear in the energy spectrum of Fig. 1) The appearance of a non-zero rhombic parameter E is due to the lift of degeneracy of the ^{4}E states as the symmetry of the complex is not exactly C$_{3v}$. The energy difference between the ground state ^{4}A$_2$ and the first excited state ^{4}A$_1$ that has a contribution to *D* is related to the energy difference between the (d$_{xz}$, d$_{yz}$) and (d$_{x^2-y^2}$, d$_{xy}$) orbitals noted ΔE$_1$, since the state ^{4}A$_1$ is obtained from a single excitation involving these orbitals. At variance, the state ^{4}E results from excitations between (d$_{xz}$, d$_{yz}$) and the d$_{z^2}$ orbitals (Fig. 1).[9, 13] In order to increase the negative contribution to *D,* the ^{4}A$_2$-^{4}A$_1$ energy difference (related to ΔE$_1$) must decrease while the ^{4}A$_2$-^{4}E energy difference (related to ΔE$_2$) must increase (Fig. 1a, and c). This effect can be achieved by designing a molecule that has longer equatorial Co-L distances (weaker equatorial σ-donating effect; L = ligand) and shorter axial Co-L bonds (larger axial σ-donating effect). These qualitative arguments only consider the σ-donating effects of the ligands, which are dominant. Increasing π-donation of the equatorial ligands will further decrease ΔE$_1$ and make *D* more negative.

Synthesis. With these parameters in mind we set out to design a ligand that would yield trigonal bipyramidal complexes with the characteristics described above. We opted for an analogue of the Me$_6$tren ligand. We replaced three nitrogen atoms with sulfur atoms, which are larger and result in longer Co-L bonds. The ligand *NS*$_3^{iPr}$ was synthesized following a modified literature procedure.[16] The general synthesis of the complex is as follows. To a solution of *NS*$_3^{iPr}$ (1 equiv.) in 1-butanol the anhydrous CoCl$_2$ salt was added (1 equiv.) to yield a purple microcrystalline solid. Air stable X-ray quality single crystals were obtained by slow evaporation of diethyl ether into a saturated ethanol/acetone (1/1) solution of [Co(*NS*$_3^{iPr}$)Cl](BPh$_4$). As expected, the ligand imposes a trigonal bipyramidal arrangement in the complexes with pseudo C$_3$ molecular symmetry axis. The cation structures is comprised of a central Co(II) ion surrounded by three sulfur atoms in the equatorial sites, a nitrogen and a chloride in the axial sites (Fig. 1).

As per design, here we show that it is possible to engineer the magnetic anisotropy (control of the magnitude of the spin Hamiltonian parameter *D*) in trigonal bipyramidal Co(II) complexes. There is a significant difference in the bond distance between [Co(*NS*$_3^{iPr}$)Cl](BPh$_4$) (Table S2) and its Me$_6$tren analogue. By replacing the ligand's equatorial nitrogen atoms with sulfur atoms, the Co-equatorial atom's distance was increased by 0.245 Å from 2.152 Å (for the [Co(Me$_6$tren)Cl](ClO$_4$) complex)[9] to 2.397 Å (average values as the three Co-S bonds have different lengths) for Co-N and Co-S, respectively. This elongation resulted in a slightly shorter Co-Cl bond distance in [Co(*NS*$_3^{iPr}$)Cl](BPh$_4$). These two effects in unison translated to a dramatic increase in the $|D|$ value, which went from -8.1 cm^{-1} for [Co(Me$_6$tren)Cl](ClO$_4$) to -19.1 cm^{-1} for [Co(*NS*$_3^{iPr}$)Cl](BPh$_4$). It is important to note that within the crystal lattice of [Co(*NS*$_3^{iPr}$)Cl](BPh$_4$) there are two geometrically different complexes that have the same pseudo trigonal bipyramidal structure with different Co-S and Co-N bond lengths (See table S1). These two different isomers have different *D* values (-23.0, and -13.1 cm^{-1} for isomers a and b respectively, see Table S1), as seen from the *ab initio* calculations. We can relate the differences to the geometry of the complexes, as described in more detail in the following sections.

DC magnetic data and EPR studies. Variable temperature d.c. magnetic susceptibility data were taken between 2 and 300 K and at 1000 and 10000 Oe (Fig. S1 and S2). The χT is constant between room temperature and 40 K, with values close to 2.4 cm^{3}mol^{-1} (Fig. S1). Below 40 K the χT decreases indicating zero-field splitting (ZFS) of the M_S = ± 1/2 and ± 3/2 sublevels (magnetic anisotropy). The magnetization (*M*) versus $\mu_0 H$ (and $\mu_0 H/T$) plots (Fig. S2) confirm the presence of magnetic anisotropy. Fitting the data using the spin Hamiltonian $H = g\beta \boldsymbol{S} \cdot \boldsymbol{B} + D[S_z^2 - S(S+1)/3] + E(S_x^2 - S_y^2)$ for S = 3/2 gives to the following values *-19.9 cm^{-1}, 1.5 cm^{-1} and 2.43* for *D*, *E, and g* parameters respectively. The spin Hamiltonian parameters obtained from the fit correspond to the two

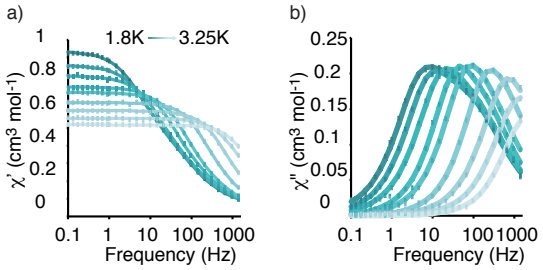

Figure 2. A.c. magnetic susceptibility data. a) χ', and b) χ'' as a function of wave frequency at T = 1.8 to 3.5 K, and d.c. applied field = 2000 Oe for [Co(NS_3^{iPr})Cl](BPh$_4$). The squares represent the experimental values, and the lines are the theoretical fits (see belopo).

crystallographically independent molecules; it is not possible from the magnetization data to differentiate them. We have thus calculated the magnetization *vs.* field curves using the spin Hamiltonian parameters obtained from the *ab initio* calculations (D = -23 and -13 cm^{-1} and E/D = 0.09) and found that the mean curves are in very good agreement with the experimental ones (Fig. S2 bottom). The theoretical barriers for the two independent molecules corresponding to the energy difference between the ground M_S = ± 3/2 and the excited M_S = ± ½ Kramers doublets are thus expected to be equal to 46 and 26 cm^{-1} (2|*D*|).

In order to validate the magnetization results, we performed a powder EPR study at several frequencies, from X-band to 662 GHz, and at temperatures ranging from 5 to 40 K. Unfortunately, the quality of the recorded spectra was rather poor even at X-band frequency, perhaps due to non-resonant absorption of the microwave power by the sulfur ligand. Thus, only a few transitions could be identified and the resulting information on the magnetic anisotropy of the system is limited. At the lowest temperature, only one signal is observed at low frequencies corresponding to an effective g-value of 7.05 (Fig. S3). With the increase of the frequency, this signal splits in two components of comparable intensity, with effective g-values of g_{1eff} = 7.14 and g_{2eff} = 6.95 respectively. These two signals originate from the ground energy level (M_S = -3/2) as their intensity decreases with the increase of temperature. Conversely, another signal appears at temperature larger than 5 K; it corresponds to an effective g-value of g_{3eff} = 3.18. From the rough temperature dependence performed (measurements at 5, 15, 25 and 40 K), the signal intensity goes through a maximum around 25 K with an uncertainty of ±10 K (Fig S3 bottom). This signal, coming from an excited level, is attributed to a transition inside the M_S = ±1/2 levels because it can be followed with an effective g description. As no other signal could be surely identified, it is not possible to extract the parameters governing the magnetic anisotropy directly from the EPR spectra. Thus, we limited the analysis to checking the compatibility with the resonances expected using the values obtained from *ab initio* calculations. Fixing the g-values, according to the magnetic measurements, to g_x = g_y = 2.2 and g_z = 2.4, we find that g_{1eff} corresponds to |E/D| = 0.09, close to the values obtained from the *ab initio* calculations. Conversely, for the same set of fixed g-values,

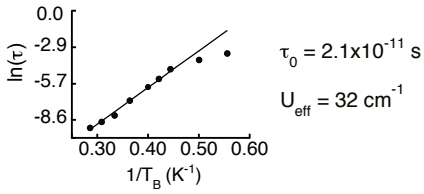

Figure 3. ln(τ) = f(1/T) for the slow relaxation processes of [Co(NS_3^{iPr})Cl](BPh$_4$).

g_{2eff} corresponds to |E/D|=0.18, far from the calculated value. However, both signals have comparable intensities, pointing towards signals associated to the different molecules present in the cell. Finally, the high-frequency EPR study allows determining a minimum value for the axial anisotropy parameter |D|, due to the absence of new signals (up to 662 GHz): |D|>15 cm^{-1}.

AC studies. To probe into the relaxation dynamics, a.c. magnetic susceptibility measurements were carried out on microcrystalline samples. The compound showed frequency dependence of the out-of phase (χ'') susceptibility and slow relaxation of its magnetization (Fig. 2) For [Co(NS_3^{iPr})Cl](BPh$_4$), the χ'' as a function of wave frequency signal (Fig. 2b) is broad. The χ'' and χ' and their corresponding cole-cole plots can then be deconvoluted into two series of curves (Fig. S4, S5 and S6). The two series of curves correspond to two sets of relaxation processes: one where the relaxation is dominated by relaxation over the energy barrier and the other where faster processes dominate. The fit of the cole-cole plots to the generalized Debye model was performed for the plots corresponding to the slower processes, which allows extracting the relaxation times (τ) and their distribution (α) for each temperature (Table S3).[17] Fitting the linear parts of the ln(τ) = f(1/T) plot (Fig. 3) provides the magnitude of the effective energy barriers for the reorientation of the magnetization U_{eff} that is found equal to 32 cm^{-1} (46 K).

Micro-SQUID magnetic data. To probe the SMM behavior of [Co(NS_3^{iPr})Cl](BPh$_4$), and to gain further insight into its low temperature behavior, single crystal magnetization measurements were performed using a micro-SQUID[18] instrument at temperatures ranging from 0.03 to 5 K. The field was aligned parallel to the easy axis of magnetization by using the transverse field method.[19] Opening of the hysteresis loops were observed below T = 2 K (Fig. 4a), indicating that the complex exhibits slow relaxation of the magnetization. The effect of the quantum tunneling of the magnetization (QTM) between the M_S = ±3/2 states is evidenced by the steps at zero field. The tunnel rate is very fast because even at our fastest field sweep rate of 0.28 T/s the hysteresis loop remains closed at $\mu_0 H$ = 0, which is consistent with the results of the aforementioned a.c. studies. In order to see better the slow relaxation at non-zero field, we recorded hysteresis loops starting from $\mu_0 H$ = 0, at 0.03 K, and with scan rates in the range of 0.004-0.280 T/s (Fig. 4b). As soon as a small field is applied, tunneling is blocked and a large amount of molecules are in the M_S = +3/2 state (instead of all the molecules being in the M_S = -3/2 expected when upon increasing the field and in the absence of blocking) and this amount decreases slowly

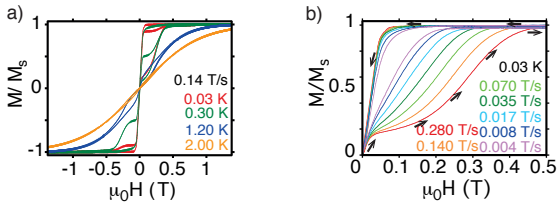

Figure 4. a) Magnetization *vs.* field on a single crystal of [Co(NS_3^{iPr})Cl](BPh$_4$) at different temperatures and fixed scan rate, and b) first magnetization curves for different sweep rates at 0.03K, obtained by cooling down the single crystal in zero field and then starting the hysteresis loop from zero field.

upon increasing the magnetic field, revealing a large SMM-type hysteresis. At higher fields, the molecules in M_S = +3/2 relaxes to the M_S = -3/2 state via the direct relaxation process, emitting a phonon.

Theoretical calculations. Theoretical calculations were performed to validate the experimental values of D obtained, as it is not possible to distinguish between the magnetism of the two independent molecules. We used the experimental geometries for our study. The *ab initio* calculations were done using the two-step approach implemented in the MOLCAS code (see SI for details).[20-24] The values of *D* are reported in Table S1 and their average is in perfect agreement with the experimental values obtained. It is worth noting that the difference in the calculated *D* values for the two isomers of [Co(NS_3^{iPr})Cl](BPh$_4$) is mainly due to the energy difference (Table S4) between the ground ($^4A_2$) and the first excited state ($^4A_1$). This energy difference between the states is related to the energy difference ΔE_1 between the (d_{xz}, d_{yz}) and the (d_{xy}, $d_{x^2-y^2}$) orbitals (Fig. 1). This effect translated to a weaker energy difference in complexes that have larger equatorial metal-ligand (Co-S) distances. We, therefore, obtain a larger $|D|$ value for [Co(NS_3^{iPr})Cl]$^+$ (a) than for [Co(NS_3^{iPr})Cl]$^+$ (b) (-23.0 and -13.1 cm^{-1}, respectively). In addition to their size sulfur atoms possess π-donating character that reduces the energy differences between $^4A_2$ and $^4A_1$, bringing an additional negative contribution to *D*. This increase of $|D|$ results in a longer relaxation time (Fig. 2) even though there is a non negligible transversal term (E) for [Co(NS_3^{iPr})Cl](BPh$_4$).

The conclusion from this work is that we can engineer and tune the anisotropy and the barrier of the reorientation of the magnetization of trigonal bipyramidal Co(II) complexes by chemical design. Despite the presence of a transverse anisotropy term in the sulfur based complexes, the effective energy barrier U_{eff} was increased from 16 cm^{-1} (CoMe$_6$trenCl$^+$) to 32 cm^{-1} in the present case. The reduction of the value of the energy barrier from the theoretical one (46 cm^{-1} corresponding the isomer with the largest |D| value) is about 30%. It is usually ascribed to multiphonon processes (Raman type) that are active at high temperatures.[11] At low temperature where the micro-Squid data were recorded, the multiphonon processes are negligible.[25] At these temperatures only direct and quantum tunneling processes are active. The fast relaxation at zero field observed in the M = f($\mu_0 H$) loops are mainly due to the nature of the wavefunctions within the Kramers low-lying doublet. The presence of a rhombic ter due to the lack of the strict axial symmetry of the complex mixes the M_S wavefunctions (-1/2 with +3/2 and +1/2 w h 3/2). The degenerate ground state Kramers doublet is not a pure ±3/2 state but has contribution from the ±1/2 wavefunctions; this mixing together with small local transver e fields (dipolar, hyperfine, etc.) opens a tunnel splitting within the ground state levels and is responsible for the fast quantu n tunneling of the magnetization at H = 0.

This work is partially financed by ANR-project MolNanoSpin 13-BS10-0001-03. Y.L and W. W. thank the EU for financial support within the FP7 FET-Proactive project MoQuaS . 610449. We thank the collaborative program between th China Scholarship Council and Université Paris-Su (No.201306310014), UPS, Région Ile de France SESAM program 2012 N°12018501, LabEx CHARM^{3}AT, and CNRS. T thanks the IUF (Institut Universitaire de France) for financial support

Notes and references

1. R. Sessoli, H. L. Tsai, A. R. Schake, S. Wang, J. B. Vincent, K. Folting, D Gatteschi, G. Christou and D. N. Hendrickson, *J. Am. Chem. Soc.*, 1993, **1**, 1804-1816.
2. A. Caneschi, D. Gatteschi, R. Sessoli, A. L. Barra, L. C. Brunel and M. Guillot *J. Am. Chem. Soc.*, 1991, **113**, 5873-5874.
3. L. Bogani and W. Wernsdorfer, *Nat. Mater.*, 2008, **7**, 179-186.
4. R. Sessoli, *Angew. Chem., Int. Ed.*, 2012, **51**, 43-45.
5. R. Sessoli, D. Gatteschi, A. Caneschi and M. A. Novak, *Nature*, 1993, **365**, 14 143.
6. N. Ishikawa, M. Sugita, T. Ishikawa, S.-y. Koshihara and Y. Kaizu, *J. Am. Che Soc.*, 2003, **125**, 8694-8695.
7. D. N. Woodruff, R. E. P. Winpenny and R. A. Layfield, *Chem. Rev.*, 2013, 511 5148.
8. J. D. Rinehart and J. R. Long, *Chem. Sci.*, 2011, **2**, 2078-2085.
9. R. Ruamps, L. J. Batchelor, R. Guillot, G. Zakhia, A.-L. Barra, W. Wernsdorfer, Guihéry and T. Mallah, *Chem. Sci.*, 2014, **5**, 3418.
10. R. Ruamps, R. Maurice, L. Batchelor, M. Boggio-Pasqua, R. Guillot, A.-L. Barra, J. Liu, E.-E. Bendeif, S. Pillet, S. Hill, T. Mallah and N. Guihéry, *J. Am. Chem Soc.*, 2013, **135**, 3017-3026.
11. J. M. Zadrozny, D. J. Xiao, M. Atanasov, G. J. Long, F. Grandjean, F. Neese and J. R. Long, *Nat. Chem.*, 2013, **5**, 577-581.
12. J. M. Zadrozny, J. Liu, N. A. Piro, C. J. Chang, S. Hill and J. R. Long, *Chem. Commun.*, 2013, **48**, 3927.
13. D. Schweinfurth, M. G. Sommer, M. Atanasov, S. Demeshko, S. Hohloch, Meyer, F. Neese and B. Sarkar, *J. Am. Chem. Soc.*, 2015, 150128161813009.
14. F. E. Mabbs and D. Collison, *Electron paramagnetic resonance of d transiti metal compounds*, Elsevier, 2013.
15. J. N. Rebilly, G. Charron, E. Rivière, R. Guillot, A. L. Barra, M. D. Serrano, J. v n Slageren and T. Mallah, *Chem.-Eur. J.*, 2008, **14**, 1169-1177.
16. G. Fallani, R. Morassi and F. Zanobini, *Inorg. Chim. Acta*, 1975, **12**, 147-154.
17. K. S. Cole and R. H. Cole, *J. Chem. Phys.*, 1941, **9**, 341-351.
18. W. Wernsdorfer, *Supercond. Sci. Technol.*, 2009, **22**, 064013.
19. N. Ishikawa, *J. Phys. Chem. A*, 2003, **107**, 5831-5835.
20. R. Maurice, R. Bastardis, C. d. Graaf, N. Suaud, T. Mallah and N. Guihéry, *Chem. Theory Comput.*, 2009, **5**, 2977-2984.
21. F. Aquilante, L. De Vico, N. Ferré, G. Ghigo, P.-Å. Malmqvist, P. Neogrády . B. Pedersen, M. Pitoňàk, M. Reiher, B. Roos, L. Serrano-Andrés, M. Urba V. Veryazov and R. Lindh, *J. Comput. Chem.*, 2010, **31**, 224-247.
22. B. O. Roos and P.-A. Malmqvist, *Phys. Chem. Chem. Phys.*, 2004, **6**, 2919-292
23. G. Karlstroem, R. Lindh, P.-A. Malmqvist, B. O. Roos, U. Ryde, V. Veryazov, O. Widmark, M. Cossi, B. Schimmelpfennig, P. Neogrady and L. Seijo, *Comp Mater. Sci.*, 2003, **28**, 222-239.
24. P. A. Malmqvist, B. O. Roos and B. Schimmelpfennig, *Chem. Phys. Lett.*, 2002 **357**, 230-240.
25. A. Abragam and B. Bleaney, *Electron paramagnetic resonance of transiti ions*, Oxford University Press, 2012.

